On the effect of partial underfilling on the fatigue life of flip-chip micro-solder bumps in a heterogeneously integrated TSI package using finite element simulations

Sasi Kumar Tippabhotla, Lin Ji
Institute of Microelectronics
A*STAR (Agency for Science, Technology, and Research)
Singapore 138634
email: sasi_kumar_tippabhotla@ime.a-star.edu.sg

***Abstract*—The requirement of partial underfilling of flip-chips in certain heterogeneously integrated packages could adversely affect the fatigue life of the micro-solder bumps. We performed numerical simulations to show that the underfilling of the surrounding regions of micro-bumps is necessary to have a comparable fatigue life as those of the full underfill case. The effect of underfill away from the micro-bumps is insignificant on their fatigue life. In the case of partial underfilling with some bumps without surrounding underfill, they become critical with significantly lower life as compared to the micro-bumps surrounded by underfill.**

Keywords—Finite Element Analysis, Partial Underfill, Solder Bump Fatigue, Heterogenous Integration, Si-interposer, System-in-Package

I. Introduction

Heterogeneous integration (HI) is an advanced packaging technology to integrate dissimilar chips into a package. In a typical 2.5D through silicon interposer (TSI) package, HI is achieved by flip-chip bonding of dissimilar chips on to a silicon interposer with through silicon vias (TSV) [1, 2]. In certain such packages, some of the dies (chips) are packed so closely due to the package design and electrical routing constraints, etc., so that some of the edges are not accessible for the underfill injector. In addition to this, some of the dies require high level of surface purity such that the underfill material should not cover those surfaces. Due to these reasons, partial underfilling is the inevitable option.

Underfill material between the interposer and the flip-chip moderates the deformation of the micro-bumps by sharing some of the thermomechanical loading due to the CTE mismatch between the interposer and the die. It is evident from the reported literature that the underfill condition [3-4] and material properties [5] affect the micro-solder bump fatigue. In this scenario, it is necessary to evaluate the effect of the extent of partial underfill on the fatigue life of the micro-bumps and relate it to a full underfill condition. The outcome of this study helps package design engineers to identify a suitable underfill material to meet the target fatigue life for the micro-bumps.

In this study a nonlinear 3D finite element model of the flip-chip on the silicon interposer with Cu stud micro-solder bumps was developed to evaluate the effect of the partial underfilling. The model was subjected to thermal cycling on board from -40 ^{o}C to 125 ^{o}C. Three different partial underfill conditions were simulated for two different micro bump layouts. The results show that the underfill significantly affects the fatigue of micro-bumps and the life of the micro-bumps without underfill is nearly one order lower compared to that with underfill. Further, the effect of the underfill surrounding the bump is very significant and removal of underfill from region away from the micro-bumps has less significant effect on the fatigue life of the micro-bumps.

II. Package Details

Fig.1 shows a 2.5D TSI package with a Cu metal cap. The die arrangement in the layout (Fig. 1(a)) is shown only for the purpose of demonstrating the need for partial underfilling. For example, the die D1 is very close to the other dies at its left side top and bottom corners. The gap between the dies here is so low that a underfill injector cannot reach that place. Similarly, some regions at the boundary of the dies are not accessible due to connector routings. In such situations, either a layout modification or partial underfilling is inevitable. If the package layout cannot be altered for some reason, partial underfilling is the only resort. In this study the die D1 is selected for the partial underfilling study.

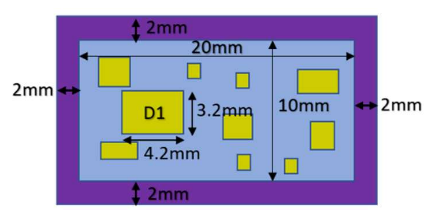

(a)

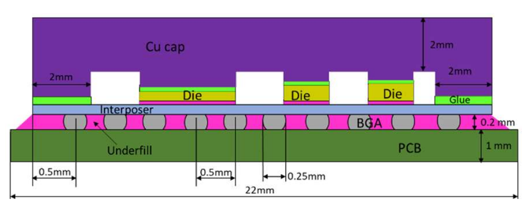

(b)

Fig. 1. Schematic of a 2.5D TSI package with a metal cap (not to the scale). (a). Package layout (metal cap top cover is not shown) (b) Typical section view of TSI package with PCB and solder bumps

The details of different layers of the package are shown in Fig. 2. Solder micro-bumps with copper studs or simply stud-bumps are used to connect the flip-chip and the interposer as shown. Though the schematic shows full underfill below the die D1, different partial underfilling conditions are modeled and studied for two different stud-bump layouts shown in the Fig. 3.

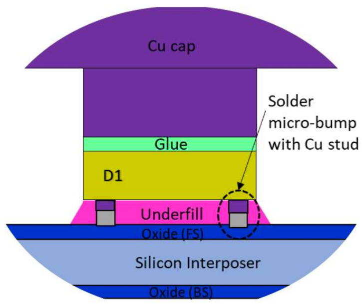

Fig. 2. Schematic of layer stack details of package (without solder bumps below interposer and PCB) shown in the Fig.1 (not to the scale)

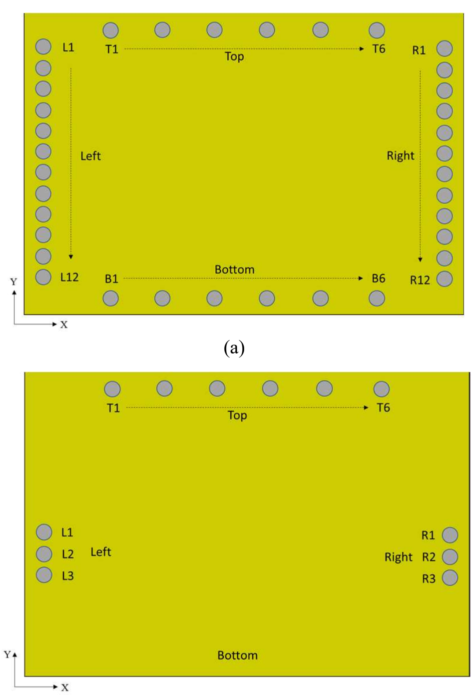

(a)

(b)

Fig. 3. Schematic of flip-chip stud-bump layout. (a) Layout-1: 36 stud-bumps, (b) Layout-2: 12 stud-bumps

III. Finite Element Modeling

A. Finite Element Mesh

Finite element model of the package is shown in Fig. 4. The model is fine meshed around the die D1, as shown in Figures 4(a) and 4(b). Stud-bumps are modeled as shown in Figures 4(c) and 4(d). Other dies are modeled with coarse mesh and stud-bumps are not modeled for them. The bigger solder bumps between the interposer and the PCB are not explicitly modeled but, represented by a uniform layer with effective material properties combining solder and underfill [6,7]. The rest of the layer structure is modeled as shown in Fig. 2. The 3D mesh is generated by extruding a 2D area mesh, hence the mesh structure for all the layers remains same, only the number of elements vary in the thickness (Z) direction.

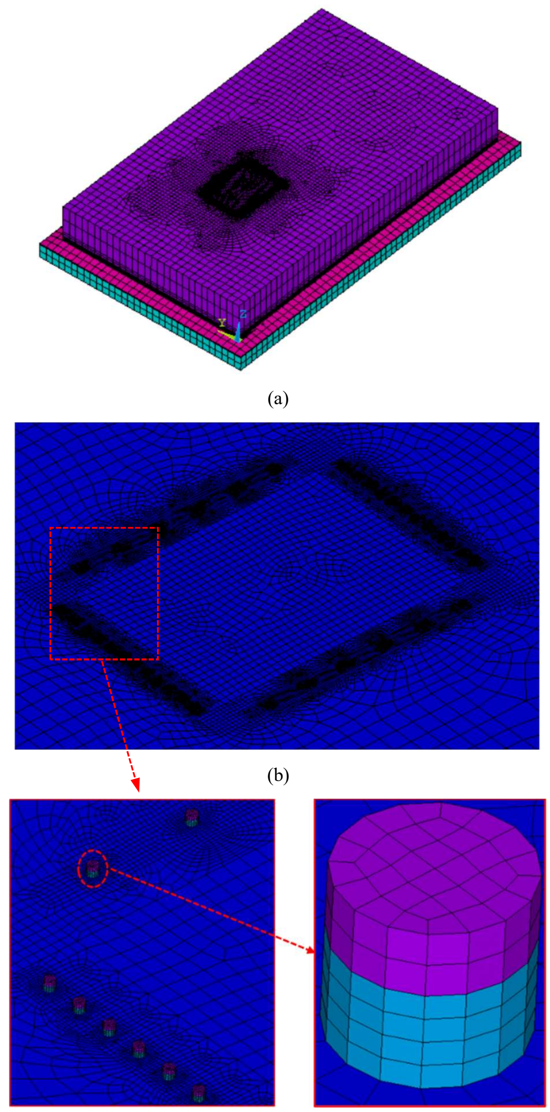

(a)

(b)

(c) (d)

Fig. 4. Finite element model details (a) full package mesh; Mesh details near, (b) Die D1, (c) stud bumps; (d) mesh of stud-bump

B. Material Properties

Table I shows the material properties used in this simulation study. All the materials except solder and PCB are assumed to be isotropic and linearly elastic. Orthotropic and linearly elastic properties are used for the PCB (FR4) material. A hyperbolic sine creep model for the Sn-Ag-Cu solder [8] is used in this study to simulate the visco-plastic creep behavior of the solder micro-bumps. Equation (1) shows the solder creep model and the corresponding material constants are given by Table II.

TABLE I. MATERIAL PROPERTIES

Component / Layer	Material	Modulus (GPa)	CTE (ppm/°C)	Poisson's Ratio	Tg (°C)
Cu Cap/Pad/Stud	Copper	117	17	0.34	-
Die	GaAs	82.7	5.73	0.3	-
Oxide	SiO_2	73	0.5	0.17	-
Interposer	Si	131	2.8	0.28	-
Polymer dielectric	Polyimide	3.5/0.1	65/500	0.3	215
Solder	Sn-Ag-Cu	54.43@-40°C 41.73@25°C 36.84@50°C 22.19@125°C	22	0.35	-
Underfill	Underfill Polymer	13/0.5	23/80	0.3	120
Solder mask	Solder mask	2.4	50	0.3	100
PCB	FR4	Ex/Ey/Ez 25/25/11	CTEx/CTEy/CTEz 18/18/35	vxy/vxz/vyz 0.11/0.39/0.39	-
Cu Cap/Die Glue	Conductive Epoxy	3.1/0.3	45/220	0.3	40

$$\dot{\varepsilon}_c = C_1[sinh(C_2\sigma)]^{C_3} exp\left(\frac{-C_4}{T}\right) \quad (1)$$

TABLE II. MATERIAL CONSTANTS OF CREEP MODEL FOR SOLDER

Constant	C_1	C_2	C_3	C_4
Value	32000	0.037	5.1	6424.7

C. Fatigue Life Prediction Model for Micro-Solder Bumps

The finite element model is subjected to the thermal cycling on board (TCOB), between -40 °C and 125 °C for 1 hour, as shown by the cycle profile in Fig. 5. Simulations are conducted for 2 thermal cycles and the accumulated creep strain energy density (W_{cr}) in the second cycle is used to evaluate the fatigue life of the solder micro-bumps, based on Schubert creep life model [9] as shown by (2).

$$N_f = 345(W_{cr})^{-1.02} \quad (2)$$

where, $W_{cr} = (W_{cr}^{avg})_{Cycle2} - (W_{cr}^{avg})_{Cycle1}$, is the creep strain energy density (SEND-Creep) accumulation in a stabilized loading cycle. As the solder micro-bump is very small, the average creep strain energy density (W_{cr}^{avg}) for each TCOB cycle for a micro-bump is calculated by averaging the elemental creep strain energy densities over the bump volume. Note that this life prediction model was actually developed for solder bumps of flip-chips on board (FCOB) and ball grid array (BGA) [9]. This model is used here to have a first order approximation and comparison of micro-bump life for different partial underfilling conditions.

Fig. 5. Thermical Cycling on Board (TCOB) Profile – 1 Cycle

D. Partial Underfilling Case Studies

As the focus of this study is to evaluate the effect of partial underfilling below the die on the fatigue life of solder stud-bumps, case studies (CS) with three different partial underfill schemes, as shown in Fig. 6 are simulated. Initially, case studies CS1, CS2 and CS3 are simulated for micro-bump layout-1 with 36 bumps (ref. Fig. 3 (a)). Based on the results, further case studies CS1, CS3, and CS4 are simulated for micro-bump layout-2 with 12 bumps (ref. Fig. 3 (b)). The results of the simulation studies are presented in following section.

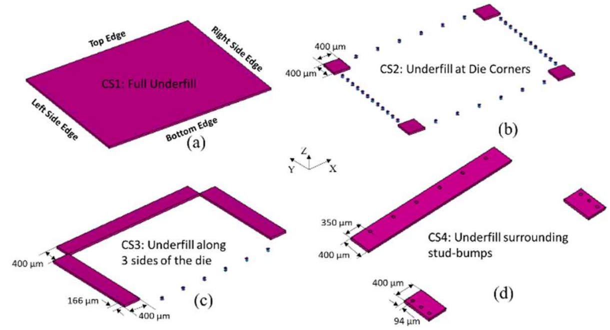

Fig. 6. Underfilling casestudies. (a) CS1: Full underfill; (b) CS2: Underfill at die corners; (c) CS3: Underfill along 3-sides of the die; (d) CS4: Underfill surrounding stud-bumps

IV. RESULTS AND DISCUSSION

Variation of peak von-Mises stress in the micro-bumps with thermal cycling time, as shown in Fig. 7 indicates that the stress peaks occur at the end of ramp-down to -40 °C. The magnitude of the stress is nearly same for 1st and 2nd thermal cycles for different cases. The stress relaxes to a lower value during dwell at -40 °C and it further decrease to a negligible value as the temperature increases back to 125 °C. Hence, von-Mises stress contours of the micro bumps at the end of ramp-down to -40 °C, for different case studies of micro-bump layout-1 are shown in Fig.8. As shown, the von-Mises stress is, ~ 53 MPa for the full underfill case (CS1), ~64 MPa for the corner underfill case (CS2), and ~61 MPa for the 3-sides underfill case (CS3). The von-Mises stress is higher for partial underfill cases (CS2 and CS3), but the difference in the stress is not very significant. Therefore, a further probe of individual stress components (normal and shear stresses in different directions) is necessary to understand the effect of the underfill on the micro-bump stress state.

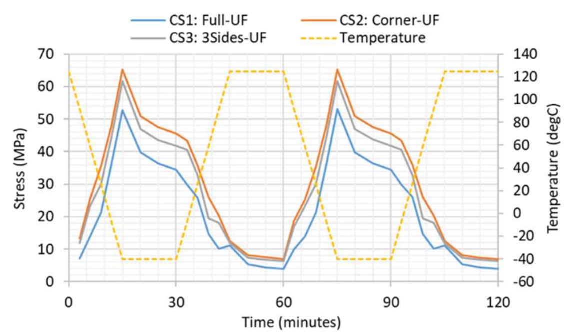

Fig. 7. Variation of von-Mises stress with cycling time for different underfill case studies (for Layout-1)

The peaks of individual stress components occur at different bumps for different cases. Hence, to have a meaningful comparison, the peak component stresses at the critical (min. fatigue life) micro-bump for different underfill cases of Layout-1 are probed and compared. The critical micro-bumps for CS1 is at R12 and that for CS2 and CS3 is at B3 (ref. Fig. 3(a)). Figure 9 shows variation of peak normal stress components of critical bump with cycling time for different underfill cases. The in-plane stresses (S_X and S_Y) are tensile 60 MPa, for the case of full underfill (CS1), significantly higher than those of the partial underfill cases (CS2 and CS3). Partial underfilling seem to reduce these tensile stresses.

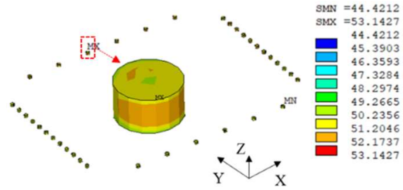

(a) CS1: Full UF

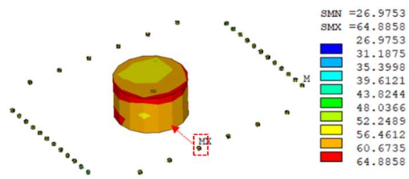

(b) CS2: Corner UF

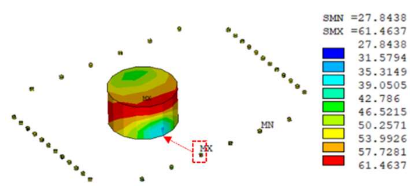

(c) CS3: 3Sides UF

Fig. 8. Von-Mises stress contours for different underfill case studies (for Layout-1)

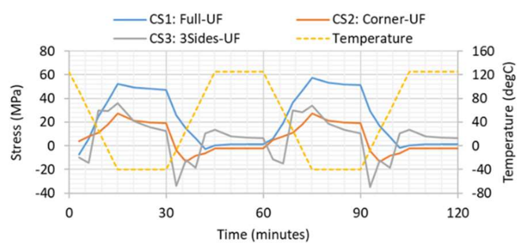

(a) Normal Stress (S_X)

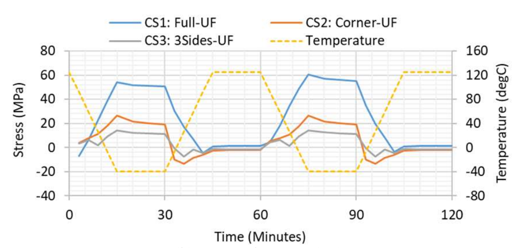

(b) Normal Stress (S_Y)

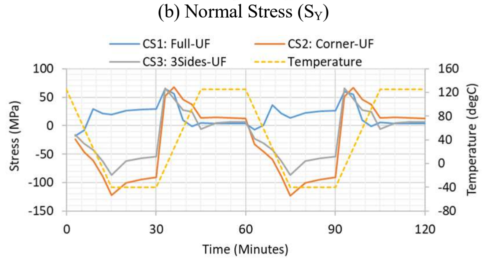

(c) Normal Stress (S_Z)

Fig. 9. Variation of normal stress components of critical bump with cycling time for different underfill case studies (for Layout-1)

The out-of-plane normal stress (S_Z) is tensile for the full underfill case (CS1) and compressive for the partial underfill cases (CS2 and CS3) and the magnitude is significantly higher (-120 MPa for CS2 and -85 MPa for CS3). Note that, for both CS2 and CS3, the critical bumps have no surrounding underfill. For CS1, the critical bump has underfill in the surrounding and it experiences tensile stress (S_Z) of 65 MPa. This indicates that the underfill surrounding the bumps changes their local stress state.

Figure 10 shows variation of peak shear stress components with cycling time for different underfill cases. All the shear stress components exhibit the similar comparison among different underfill cases. The shear stress is lower for the full underfill case (CS1) and higher for the partial underfill cases (CS2 and CS3), proportional to the amount of partial underfill. This is reasonable, as the underfill reduces the CTE mismatch load on the bumps by sharing it.

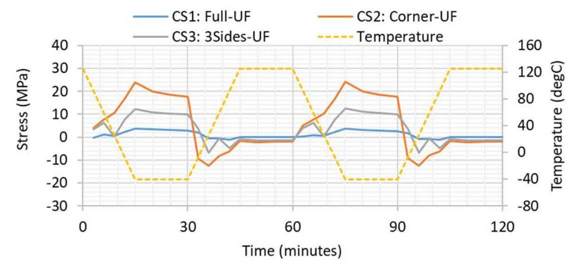

(a) Shear Stress (S_{XY})

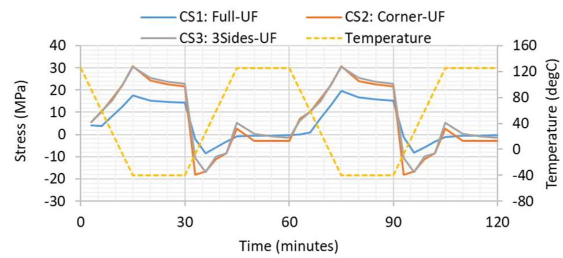

(b) Shear Stress (S_{YZ})

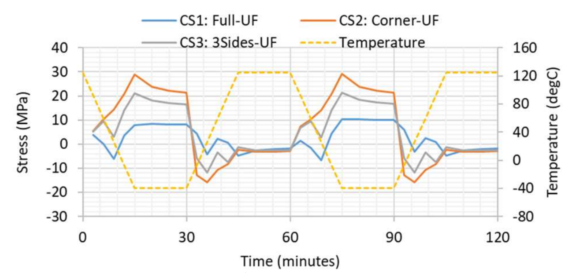

(c) Shear Stress (S_{XZ})

Fig. 10. Variation of shear stress components of critical bump with cycling time for different underfill case studies (for Layout-1)

The in-plane shear stress (S_{XY}) is negligible (4 MPa) for CS1, 24 MPa for CS2 and 10 MPa for CS3. As this is in-plane shear, the entire underfill area contributes the reduction of stress on the micro-bump. Therefore, the stress for each case is nearly proportional to the amount of underfill used. The out-of-pane shear stresses (S_{YZ} and S_{XZ}) are also low, 20 MPa and 10 MPa, respectively for CS1. For the corner underfill case (CS2), these shear stress components are significantly higher (30 MPa), as there is very low volume of underfill only at the die corners, the area supporting the out-of-pane shear loads is much lower. For the case of 3-sides underfill (CS3), S_{YZ} is 30

MPa (same as CS2), as this component is supported by underfill along the top edge of the die only. S_{XZ} for CS3 is 20 MPa, as this component is supported by underfill along 2 sides (left and sides of the die). This indicates that both the volume and layout of the partial underfill affect the micro-bump shear stress. In summary, the stress analysis revealed that, in the triaxial stress state in a micro-bump depends on the surrounding underfill. The life results in the following plots show that the bumps without surrounding underfill becomes critical.

The creep strain energy density (SEND-Creep) contours in the micro-bumps at the end of the second TCOB cycle are shown in Fig. 11. The SEND-Creep for bumps with corner underfill (CS2) is nearly 20 times high compared to the bumps with full underfill (CS1). That for the 3-sides underfill case (CS3) is nearly 10 times higher. In both these cases, the bump with max SEND-Creep is not surrounded by the underfill. Therefore, the bump fatigue is inversely proportional to the total volume of the underfill dispensed below the die.

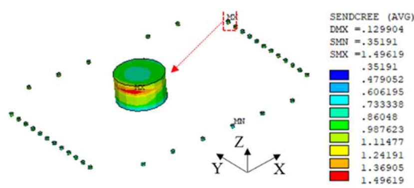

(a) CS1: Full UF

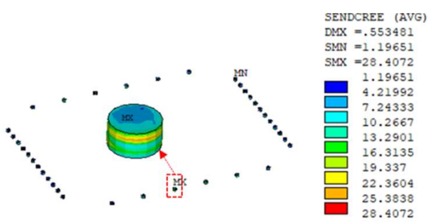

(b) CS2: Corner UF

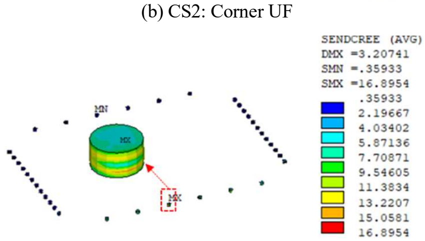

(c) CS3: 3Sides UF

Fig. 11. Creep strain energy density contours for different underfill case studies (for Layout-1)

Figure 12 shows micro-bump fatigue life for all the bumps in Layout-1. Note that the bump fatigue life is normalized by the maximum bump fatigue life of the full underfill case (CS1). Considering the Left, Right and Top side bumps, the fatigue life is comparable for full underfill case (CS1) and 3-sides underfill case (CS3). Whereas the fatigue life for corner underfill case (CS2) is nearly one order low. Further, In the case of bottom side bumps, both the corner underfill (CS2) and 3-sides underfill (CS3) have low life compared to the full underfill case (CS1). Both these observations clearly indicate that the effect of the underfill on the micro-bump life is quite significant and the partial underfill may be sufficient to achieve higher bump life, provided that the micro-bumps are fully surrounded by the underfill. The fatigue life for left and right sided bumps shows an increasing trend towards the interior of the die for the 3-sides underfill case (CS3). This is predominantly due to the availability of more surrounding material for the interior bumps. There is a small contribution due to the variation of the constraints from the die and the interposer at a particular bump. The full underfill case (CS1) also shows a similar but feeble variation.

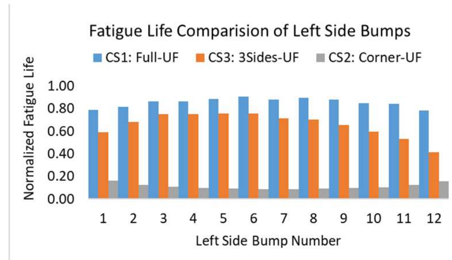

(a)

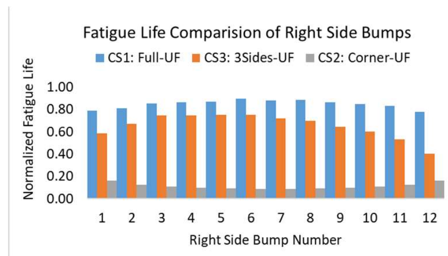

(b)

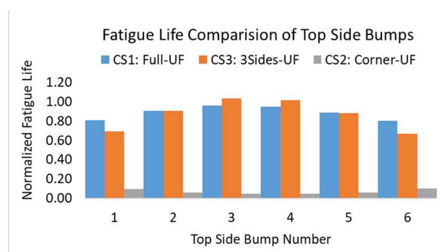

(c)

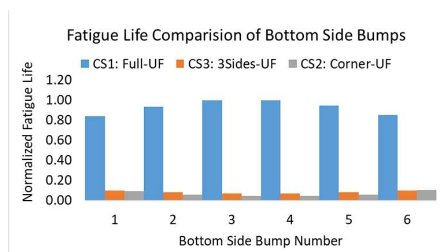

(d)

Fig. 12. Normalized fatigue life of different underfill case studies (for Layout-1). Note: the bump fatigue life is normalized by the maximum bump fatigue life of the full underfill case (CS1)

Simulation results for Layout-2 are similar to the results for Layout-1. Hence, only the fatigue life comparison of the micro-bumps is presented in Fig. 13 for brevity. As shown in Figures 13(a) and 13(b), the left side right side bumps have comparable fatigue life for the full underfill case (CS1), 3-sides underfill case (CS3) and the underfill surrounding bumps case (CS4). However, the bump life for CS4 is the lowest due to low volume of underfill on the sides. Therefore, the fatigue life decreases if the micro-bump is not surrounded by the underfill to a sufficient distance. In the case of top side bumps, as shown in Fig. 13 (c), the fatigue life is same for 3-sides underfill case (CS3) and the underfill surrounding bumps case (CS4), as the volume of the underfill surrounding the row of bumps is same for these cases. Furthermore, the fatigue life for these two cases is comparable with the full underfill case. Note that there are no bumps at the bottom side edge of the die for Layout-2.

Overall, the case studies presented in this simulation study confirm that the underfill helps to reduce the fatigue of the micro-bumps by sharing CTE mismatch loads. Secondly, sufficient volume of partial underfilling surrounding the bumps leads to the same effect as the full underfill case. In this study, for this package and solder micro-bump design, we found that the partial underfilling to 0.4 mm, from the center of the micro-bump or last micro-bump in a row, gives comparable bump fatigue life as that of the full underfill case.

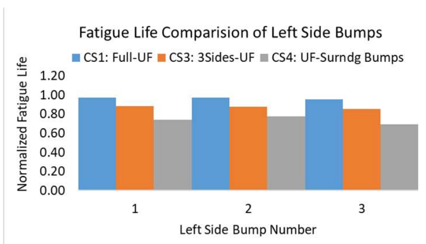

(a)

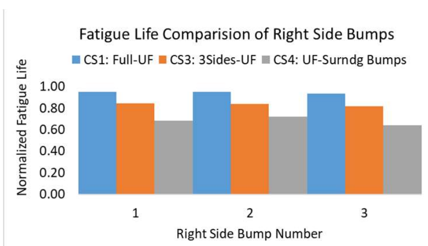

(b)

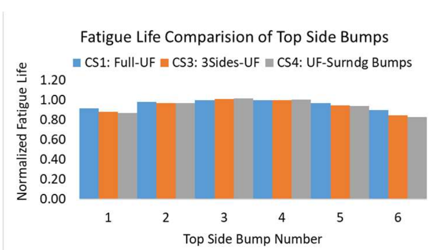

(c)

Fig. 13. Normalized fatigue life of different underfill case studies (for Layout-2). Note: the bump fatigue life is normalized by the maximum bump fatigue life of the full underfill case (CS1)

V. Conclusions

Nonlinear 3D finite element simulations of a 2.5D TSI package, with flip-chips and a metal cap, under TCOB loading, are performed to evaluate the effect of partial underfilling on the fatigue life of Cu stud solder micro-bumps. The results indicate that the underfilling helps to reduce fatigue loading on the micro-bumps, which agrees with the reviewed literature [3-5].

In the case of full underfill (CS1), all the micro-bumps are surrounded by the underfill, hence, the shear stresses are low and the stress in the critical bump is predominantly tensile. The variation of fatigue life among the micro-bumps is very minimal and this is the ideal case.

In the case of partial underfill (CS2, CS3, and CS4), the fatigue life of the bumps with surrounding underfill is high, and comparable to that of the full underfill case (CS1). Whereas for the bumps without underfill, the fatigue life is very small compared to that of the CS1. The overall stress state of the critical bumps is significantly different from the micro-bumps with underfill in this case. They are subjected to significantly higher magnitude of shear and normal stresses. As the creep strain rate is very sensitive to the magnitude of stress at high magnitudes of stress [10], these bumps have much higher creep strain energy accumulation in a small number of cycles, thus a very low fatigue life. Hence, we recommend underfill surrounding all the critical micro-bumps of the die. For the package in this study, we found that surrounding underfill to 0.4 mm, from the center of a micro-bump (or last bump in a row), gives comparable results with the full underfill case.

Finally, this study reveals that the stress state in the micro-bumps depend on the surrounding underfill. It is established that partial underfilling surrounding bumps may be sufficient to get similar micro-bump fatigue life as the full underfill case. It is further shown that this effect is insensitive to the changes in the layout of micro-bumps. The volume of the underfill away from the bump surroundings may not significantly contribute to their fatigue life.

The findings in this study are also expected to be very useful for the general cases where partial underfilling is inevitable, to plan the volume, material, and layout of partial underfilling to optimize the fatigue life of micro-bumps.

Acknowledgment

This research/project is supported by the National Research Foundation, Singapore (NRF) under NRF's Medium Sized Centre: Singapore Hybrid-Integrated Next-Generation μ-Electronics (SHINE) Centre funding programme. Any opinions, findings and conclusions or recommendations expressed in this material are those of the author(s) and do not reflect the views of the National Research Foundation, Singapore.

References

[1] F. X. Che, X. Zhang, J-K Lin, "Reliability study of 3D IC packaging based on through-silicon interposer (TSI) and silicon-less interconnection technology (SLIT) using finite element analysis", Microelectronics Reliability 61 (2016) 64–70.

[2] H. Chen, T. G. Lim and G. Tang, "Thermal Challenges and Design Considerations in Heterogeneous Integrated Through-Silicon-interposer Platform for III-V HEMT Flip Chip," 2022 IEEE 72nd Electronic Components and Technology Conference (ECTC), 2022, pp. 1030-1035.

[3] C. S. Selvanayagam, J. H. Lau, X. Zhang, S. K. W. Seah, K. Vaidyanathan, T. C. Chai, "Nonlinear Thermal Stress/Strain Analyses of Copper Filled TSV (Through Silicon Via) and Their Flip-Chip Microbumps", 58th IEEE Electronic Components and Technology Conference (ECTC), 2008, pp. 1073-1081.

[4] C. -H. Chuang, W. -H. Li, C. -H. Wang and S. -L. Lee, "Parametric study of flip chip packaging for MEMS device with diaphragm," 2010 Symposium on Design Test Integration and Packaging of MEMS/MOEMS (DTIP), 2010, pp. 362-365.

[5] J. H. Okura, K. Darbha, S. Shetty, A. Dasgupta and J. F. J. M. Caers, "Guidelines to select underfills for flip chip on board assemblies," 1999 Proceedings. 49th Electronic Components and Technology Conference (Cat. No.99CH36299), 1999, pp. 589-594.

[6] F.X. Che, L. Xie, Z.H. Chen, Sunil Wickramanayaka, "Study on Warpage and Stress of TSV Wafer with Ultra-Fine Pitch Vias for High Density Chip Stacking", in Proceedings of Electronics Packaging Technology Conference (EPTC), Singapore, 2017.

[7] F.X. Che, H.Y. Li, X.W. Zhang, S. Gao, K.H. Teo, "Development of Wafer-Level Warpage and Stress Modeling Methodology and Its Application in Process Optimization for TSV Wafers", IEEE Transactions On Components, Packaging And Manufacturing Technology (CPMT), Vol. 2, No. 6, June 2012, pp.944-955.

[8] H. L. J. Pang, B. S. Xiong, and T. H. Low, "Creep and fatigue characterization of lead free 95.5Sn-3.8Ag-0.7Cu solder," in Proc. 54th Electron.Compon. Technol. Conf., 2004, pp. 1333–1337

[9] A. Schubert, R. Dudek, E. Auerswald, A. Gollhardt, B. Michel, and H. Reichl, "Fatigue life models for SnAgCu and SnPb solder joints evaluated by experiments and simulation," in Proc. 53rd Electron. Compon. Technol. Conf., 2003, pp. 603–610.

[10] F. X. Che, "Material Characterization and Low Cycle Fatigue Model of Low Ag Content Lead-Free Solder", IEEE Transactions On Device and Materials Reliability (TDMR), Vol. 17, No. 2, June 2017, pp.298-306.